

Tensor Temperature and Shockwave Stability in a Strong Two-Dimensional Shockwave.

Wm. G. Hoover and Carol G. Hoover

Ruby Valley Research Institute

Highway Contract 60, Box 598, Ruby Valley 89833, NV USA

(Dated: April 1, 2019)

Abstract

The anisotropy of temperature is studied here in a strong two-dimensional shockwave, simulated with conventional molecular dynamics. Several forms of the kinetic temperature are considered, corresponding to different choices for the local instantaneous stream velocity. A local particle-based definition omitting any “self” contribution to the stream velocity gives the best results. The configurational temperature is not useful for this shockwave problem. Configurational temperature is subject to a shear instability and can give local negative temperatures in the vicinity of the shock front. The decay of sinusoidal shockfront perturbations shows that strong two-dimensional planar shockwaves are stable to such perturbations.

PACS numbers: 02.70.Ns, 45.10.-b, 46.15.-x, 47.11.Mn, 83.10.Ff

Keywords: Thermostats, Stress, Molecular Dynamics, Computational Methods, Smooth Particles

I. INTRODUCTION

Shockwaves are useful tools for the understanding of material behavior far from equilibrium^{1,2,3,4}. The high-pressure physicist Percy Bridgman played a key role in the adaptation of experimental shockwave physics to the thermodynamic characterization of materials at high pressure⁴. Because shockwaves join two purely equilibrium states, shown to the left and right of the central shockwave in Figure 1, the experimental and computational difficulties associated with imposing nonequilibrium boundary conditions are absent.

Begin by assuming that the flow is both stationary and one-dimensional. Such a flow gives conservation of the mass, momentum, and energy fluxes throughout the shockwave. Thus the fluxes of mass, momentum, and energy,

$$\rho u, P_{xx} + \rho u^2, \rho u[e + (P_{xx}/\rho) + (u^2/2)] + Q_x ,$$

are constant throughout the system, even in the far-from-equilibrium states within the shockwave. Here u is the flow velocity, the velocity in the x direction, the direction of propagation. We use conventional notation here, ρ for density, P for the pressure tensor, e for the internal energy per unit mass, and Q_x for the component of heat flux in the shock direction, x . It is important to recognize that both the pressure tensor and the heat flux vector are measured in a local coordinate frame moving with the local fluid velocity $u(x)$.

In a different “comoving frame”, this time moving with the shock velocity and centered on the shockwave, cold material enters from the left, with speed u_s (the “shock speed”) and hot material exits at the right, with speed $u_s - u_p$, where u_p is the “piston speed”. Computer simulations of shockwaves, using molecular dynamics, have a history of more than 50 years, dating back to the development of fast computers^{5,6,7,8,9,10,11}. Increasingly sophisticated high-pressure shockwave experiments have been carried out since the Second World War¹².

In laboratory experiments it is convenient to measure the two speeds, u_s and u_p . These two values, together with the initial “cold” values of the density, pressure, and energy, make it possible to solve the three conservation equations for the “hot values” of ρ , P_{xx} , and e . A linear relation between $P_{xx}(x)$ and $V(x) = 1/\rho$, results when the mass flux $M \equiv \rho u$ is substituted into the equation for momentum conservation:

$$P_{xx}(x) + M^2/\rho(x) = P_{\text{hot}} + (M^2/\rho_{\text{hot}}) = P_{\text{cold}} + (M^2/\rho_{\text{cold}}) .$$

Figure 1

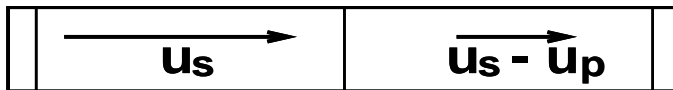


Figure 1: A stationary one-dimensional shockwave. Cold material enters at the left with a speed u_s , passes through the shockfront which separates the cold material from the hot, and exits at the right with speed $u_s - u_p$. The cold-to-hot conversion process is irreversible and corresponds to an overall entropy increase.

This nonequilibrium pressure-tensor relation is called the “Rayleigh Line”. The energy conservation relation,

$$\Delta e = -(1/2)[P_{\text{hot}} + P_{\text{cold}}]\Delta V ,$$

based on equating the work of compression to the gain in internal energy, is called the “Shock Hugoniot Relation”. See Figure 2 for both. A recent comprehensive review of shockwave physics can be found in Ref. 3.

Laboratory experiments based on this approach have detailed the equations of state for many materials. Pressures in excess of 6TPa (sixty megabars) have been characterized¹². If a constitutive relation is assumed for the nonequilibrium anisotropic parts of the pressure tensor and heat flux, the conservation relations give ordinary differential equations for the shockwave profiles. With Newtonian viscosity and Fourier heat conduction the resulting “Navier-Stokes” profiles have shockwidths on the order of the mean free path^{7,8}.

Early theoretical analyses of shockwaves emphasized solutions of the Boltzmann equation. Mott-Smith’s approximate solution of that equation¹³, based on the weighted average of two equilibrium Maxwellian distributions, one hot and one cold, revealed a temperature maximum (and a corresponding entropy maximum) at the shock center, for shocks with a Mach number exceeding two. The Mach number is the ratio of the shock speed to the sound speed. Twenty years later, molecular dynamics simulations showed shockwidths of just a few atomic diameters.^{5,6,7,8} These narrow shockwaves agreed nicely with the predictions of the Navier-Stokes equations for relatively weak shocks. At higher pressures there is a tendency for the Navier-Stokes profiles to underestimate the shockwidth. Some of the computer simulations have shown the temperature maximum at the shock front predicted by Mott-Smith^{8,10}. These temperature maxima are constitutive

Figure 2

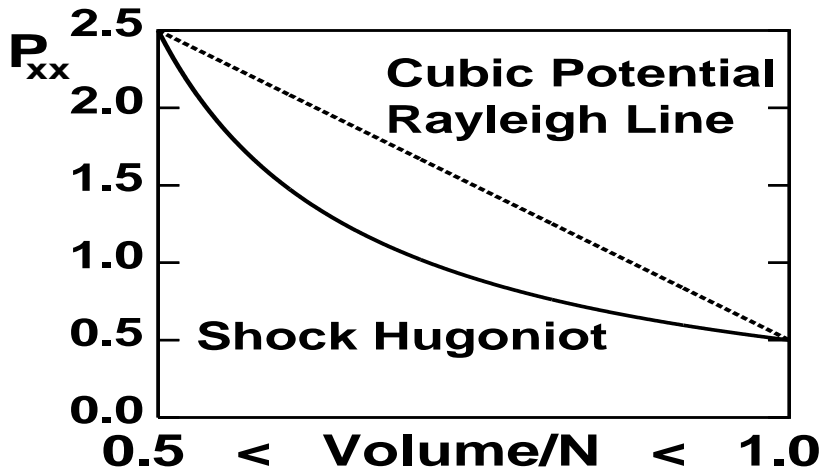


Figure 2: Calculated Rayleigh Line and Shock Hugoniot relation for the simple repulsive van der Waals' equation described in the text. The Rayleigh line includes nonequilibrium states within the shock while the Shock Hugoniot line is the locus of all equilibrium states accessible by shocking the initial state.

embarrassments — they imply a negative heat conductivity for a part of the shockwave profile.

Our interest here is twofold. We want to check on the stability of planar shockwaves (the foregoing analysis assumes this stability) and we also want to characterize the anisotropy of temperature in the shock. This latter topic is particularly interesting now in view of the several definitions of temperature applied to molecular dynamics simulations^{8,9,14,15,16,17,18}. A configurational-temperature definition as well as several kinetic-temperature definitions can all be applied to the shockwave problem.

The plan of the present work is as follows. Section II describes the material model and computational setup of the simulations. Section III describes the computation of the shock profiles and the analysis confirming their stability. Section IV compares the various kinetic and configurational temperature definitions for a strong stable shockwave. Section V details our conclusions.

II. SHOCKWAVE SIMULATION FOR A SIMPLE MODEL SYSTEM

We simulate the geometry of Figure 1 by introducing equally-spaced columns of cold particles from a square lattice. The initial lattice moves to the right at speed u_s . The interior of the system is purely Newtonian, without any boundary, constraint, or driving forces. Those particles coming within the range of the forces ($\sigma = 1$) of the righthand boundary have their velocities set equal to $u_s - u_p$ (the mean exit velocity) and are discarded once they reach the boundary. This boundary condition, because it corresponds to a diffusive heat sink at the exit, only affects the flow in the vicinity of that boundary. We initially chose the speeds $u_s = 2$ and $u_p = 1$ to correspond to twofold compression. The approximate thermal and mechanical equations of state,

$$e = (\rho/2) + T ; P = \rho e .$$

together with the initial values,

$$\rho_{\text{cold}} = 1 ; T_{\text{cold}} = 0 ; P_{\text{cold}} = (1/2) ; e_{\text{cold}} = (1/2) ,$$

give corresponding “hot” values. These two sets of thermodynamic data mutually satisfy the Rayleigh Line and Shock Hugoniot Relation for twofold compression from the cold state:

$$\rho_{\text{hot}} = 2 ; T_{\text{hot}} = (1/4) ; P_{\text{hot}} = (5/2) ; e_{\text{hot}} = (5/4) .$$

The mass, momentum, and energy fluxes are 2, $(9/2)$, and 6, respectively. For reasons explained below it was necessary to modify these conditions slightly, using instead $u_s = 2u_p = 1.75$.

We considered a wide variety of system lengths and widths and found no significant difference in the nature of the results. For convenience we show here results for a system of length $L_x = 200$ and width $L_y = 40$. Because the density increases by a factor of two in the center of the system the number of particles used in this case is about 12000. The number varies during the simulation as new particles enter and old ones are discarded. The total length of the run is one shock traversal time, $200/u_s$, though the shock is itself localized near the center of the system and in fact moves very little in our chosen coordinate frame. In retrospect, the simulations could just as well have been carried out with a much smaller L_x . Because we wished to study stability we felt it necessary to use a relatively wide system.

For a two-dimensional classical model with a weak van der Waals' repulsion the equation of state described above follows from the simple canonical partition function:

$$Z^{1/N} \propto VT e^{-\rho/2T} ; PV/NkT = [\partial \ln Z / \partial \ln V]_T ; E/NkT = [\partial \ln Z / \partial \ln T]_V .$$

Our original intent was to use the smooth repulsive pair potential¹⁹

$$\phi = (10/\pi\sigma^2)[1 - (r/\sigma)]^3 \text{ for } r < \sigma \longrightarrow$$

$$\langle \Phi \rangle \simeq (N\rho/2) \int_V \phi(r) 2\pi r dr = N\rho/2 .$$

for a sufficiently large σ (3 or so) that the simple equation of state was accurate. But for large σ the shockwidth is also so large that detailed studies are impractical. In the end we chose to set the range of the forces equal to unity, so that the initial pressure is actually zero rather than $1/2$. Nevertheless, the choice of $u_s = 2$ is still roughly compatible with twofold compression. Equilibrium molecular dynamics simulations for $\sigma = 1$ give the following solution to the conservation relations for twofold compression, from $\rho_0 = 1$ to $\rho = 2$ with $u_s = 2u_p = 1.75$:

$$\rho u : 1.0 \times 1.75 = 2.0 \times 0.875 = 1.75 ;$$

$$P + \rho u^2 : 0.0 + 1.0 \times 1.75^2 = 1.531 + 2.0 \times 0.875^2 = 3.062 ;$$

$$\rho u [e + (P/\rho) + (u^2/2)] = 1.75[0.0 + 0.0 + 1.531] = 1.75[0.383 + 0.766 + 0.383] = 1.75 \times 1.531 .$$

We introduced a sinusoidal perturbation in the initial conditions by using twice as many columns of particles (per unit length) to the right of a line near the center of the system:

$$x_{\text{shock}} = 6 \sin(2\pi y/L_y) .$$

The time development of a system starting with this sinewave displacement perturbation is shown in Figure 3. The panel corresponding to the time $t = Dt$ shows that the decay is underdamped, while the following panels show that the planar shockwave is stable.

Figure 4 illustrates the effect of the gradual underdamped flattening of the sinewave perturbation on the density profile. The propagation of the wave is followed through five shock traversal times of the observation window used in Figure 3.

The density profiles are computed with Lucy's one-dimensional weighting function^{20,21}

$$w^{1D}(r < h) = (5/4h)[1 - 6(r/h)^2 + 8(r/h)^3 - 3(r/h)^4] ; r < h = 3$$

Figure 3

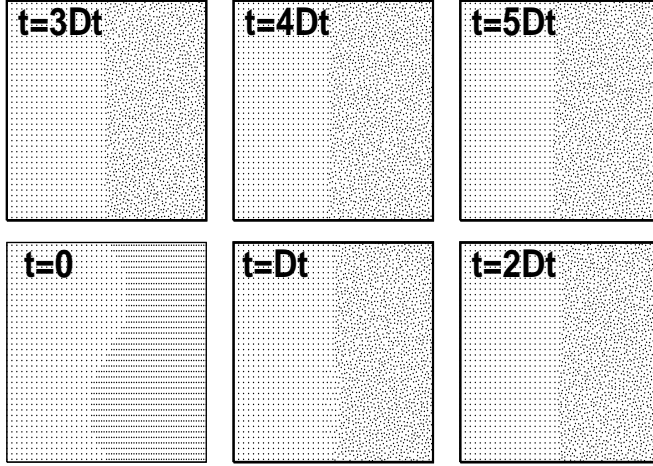


Figure 3: Particle positions in the initial condition correspond to $t = 0$. Those to the left of the sinewave boundary move to the right at speed $u_s = 1.75$ while those to the right travel at speed $u_s - u_p = u_s/2$. Particle positions at five later equally-spaced times are shown too. The time interval $Dt = 40/u_s$ is 2000 timesteps. The 40×40 windows shown here would contain 1600 cold particles or 3200 hot particles at the cold and hot densities of 1.0 and 2.0.

Figure 4

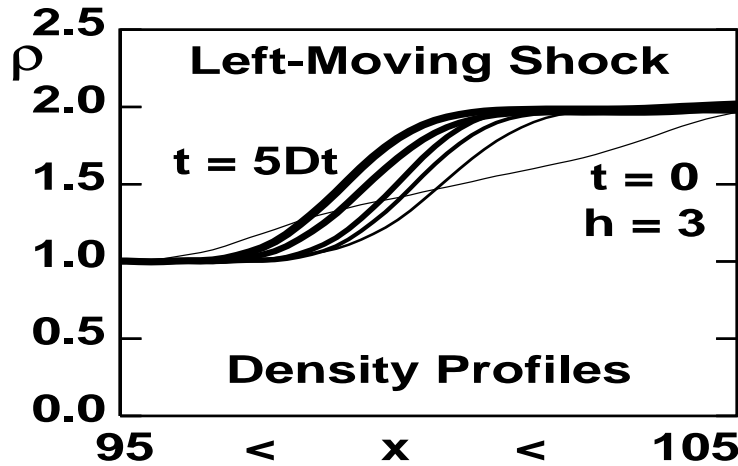


Figure 4: Density profiles at the same times as those illustrated in Figure 3. These one-dimensional density profiles were computed with Lucy's one-dimensional smooth-particle weight function using $h = 3$ and the particle coordinates shown in Figure 3. Increasing time corresponds to increasing line thickness as the shockwave moves slowly to the left.

Figure 5

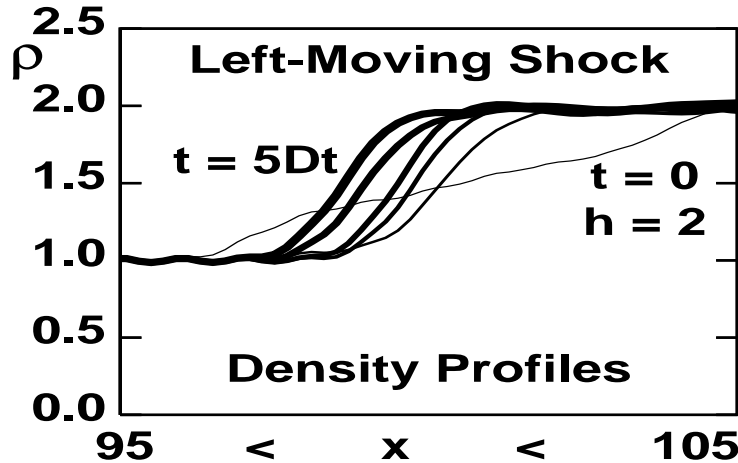


Figure 5: Density profiles exactly as in Figure 4, but with a reduced range, $h = 2$. The shockwave moves slowly to the *left*. Note the wiggly structure, a consequence of choosing h too small..

$$\rightarrow \int_{-h}^{+h} w(r) dr \equiv 1 .$$

The density is computed by evaluating the expression

$$\rho(x_k) = \sum w_{ik}^{1D} / L_y ; w_{ik}^{1D} \equiv w^{1D}(|x_i - x_k|) ,$$

for all combinations of Particle i and gridpoint k separated by no more than $h = 3$. For comparison density profiles using a shorter range, $h = 2$, are shown in Figure 5. These latter profiles exhibit a wiggly structure indicating a deterioration of the averaging process.

Similar conclusions, using similar techniques, have been drawn by Hardy and his coworkers^{9,11}, who were evidently unaware of Lucy and Monaghan's work. In their interesting analysis of a two-dimensional shockwave, Root, Hardy, and Swanson use a weight function like Lucy's, but with square (rather than circular) symmetry and with only a single vanishing derivative at its maximum range¹¹. They discuss the ambiguities of determining temperature away from equilibrium and rightly conclude that the range of the spatial weight function needs careful consideration. Hardy⁹ recently told us that his use of a spatial weighting function was motivated by a conversation with Philippe Choquard.

The profiles we show in Figure 4 are typical, and show that the shockwidth rapidly attains a value of about 3 particle diameters, and has no further tendency to change

as time goes on. A detailed study shows that the sinewave amplitude exhibits underdamped oscillations on its way to planarity. Evidently, for this two-dimensional problem, the one-dimensional shockwave structure is stable. In the next Section we consider the temperature profiles for the stationary shockwave.

III. CONFIGURATIONAL AND KINETIC TEMPERATURES IN THE SHOCKWAVE

The kinetic and configurational contributions to temperature and pressure have been discussed and explored in a variety of nonequilibrium contexts. Shockwaves, with stationary boundary conditions far from the shockfront, allow the anisotropy of the kinetic temperature to be explored, analyzed, and characterized with purely Newtonian molecular dynamics. Kinetic-theory temperature is based on the notion of an equilibrium ideal gas thermometer^{22,23,24}. The temperature(s) measured by such a thermometer are given by the second moments of the velocity distribution:

$$\{kT_{xx}^K, kT_{yy}^K\} = m\{\langle v_x^2 \rangle, \langle v_y^2 \rangle\}$$

where the velocities are measured in the comoving frame, the frame moving at the mean velocity of the fluid.

A dilute Maxwell-Boltzmann gas of small hard parallel cubes undergoing impulsive collisions with a large test particle provides an explicit model tensor thermometer for the test-particle kinetic temperature²⁴. The main difficulty associated with kinetic temperature lies in estimating the mean stream velocity, with respect to which thermal fluctuations define kinetic temperature. In what follows we compare several such definitions, in an effort to identify the best approach.

Configurational temperature is more complicated and lacks a definite microscopic mechanical model of a thermometer able to measure it. Configurational temperature is based on linking two canonical-ensemble equilibrium averages, as was written down by Landau and Lifshitz more than 50 years ago²⁵:

$$\{kT_{xx}^\Phi, kT_{yy}^\Phi\} = \{\langle F_x^2 \rangle / \langle \nabla_x^2 \mathcal{H} \rangle, \langle F_y^2 \rangle / \langle \nabla_y^2 \mathcal{H} \rangle\} .$$

\mathcal{H} is the Hamiltonian governing particle motion. Unlike kinetic temperature this configurational definition is independent of stream velocity. Its apparent dependence on

Figure 6

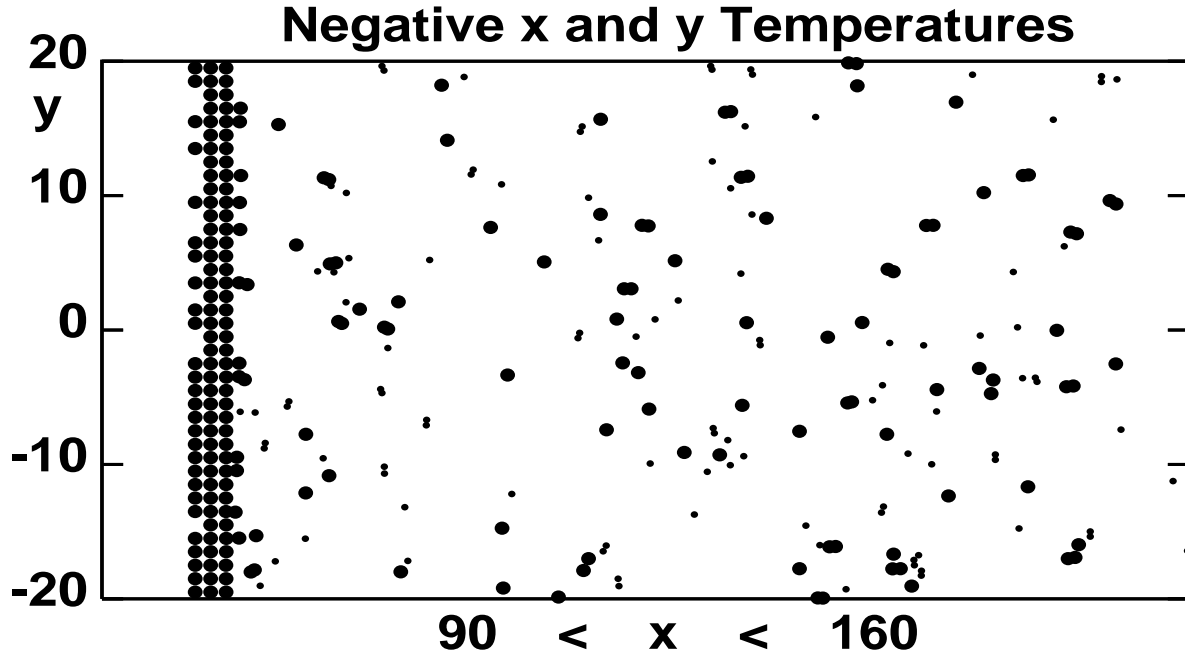


Figure 6: Particles with *negative* configurational temperatures are shown here, using the data underlying Figs. 4 and 5. The material to the right of the shock is “hot”, with cold material entering at the left. The smaller dots correspond to negative values of T_{xx}^Φ and the larger ones to negative T_{yy}^Φ .

rotation¹⁹ is negligibly small for the (irrotational) shockwave problems considered here. We apply both the kinetic and the configurational approaches to temperature measurement here, considering individual degrees of freedom within a nominally one-dimensional shockwave in two-dimensional plane geometry.

Although the notion of configurational temperature can be defended at equilibrium, the shockwave problem indicates a serious deficiency in the concept. An isolated row or column of particles, all with the same y or x coordinate and interacting with repulsive forces is clearly unstable to transverse perturbations. The symptom of this instability is a negative “force constant”

$$(\langle \nabla \nabla \mathcal{H} \rangle)_{xx \text{ or } yy} < 0 .$$

The uncertain sign of $\nabla \nabla \mathcal{H}$ explains the presence of wild fluctuations, and even negative configurational temperatures, in the vicinity of the shockfront. See Fig. 6. This outlandish behavior means that the configurational temperature is not a useful concept for such problems.

Defining the kinetic temperature requires first of all an average velocity, about which the thermal fluctuations can be computed. The velocity average can be a one-dimensional

sum over particles $\{i\}$ sufficiently close to the gridpoint k :

$$u(x_k) \equiv \sum_i w_{ik}^{1D} v_i / \sum_i w_{ik}^{1D} \longrightarrow T^{1D} .$$

Alternatively a local velocity can be defined at the location of each particle i by using a two-dimensional Lucy's weight function,

$$w^{2D}(r < h) = (5/\pi h^2)[1 - 6(r/h)^2 + 8(r/h)^3 - 3(r/h)^4] ; r < h = 3 .$$

$$\longrightarrow \int_0^h 2\pi r w(r) dr \equiv 1 ,$$

and summing over nearby particles $\{j\}$:

$$u(x_i) \equiv \sum_j w_{ij}^{2D} v_j / \sum_j w_{ij}^{2D} \longrightarrow T^{2D} .$$

These latter two-body sums can either both include or both omit the “self” term with $i = j$. Our numerical results support the intuition that it is best to omit both the self terms¹⁷. We compute all three of these x and y temperature sets for the stationary shockwave profile and plot the results in Figure 7 and 8.

The data show that in every case T_{xx} exceeds T_{yy} in the leading edge of the shock front. There is a brief time lag between the leading rise of the longitudinal temperature T_{xx} and the consequent rise of the transverse temperature T_{yy} . This is to be expected from the nature of the shock process, which converts momentum in the x direction into heat^{26,27}. The Rayleigh line itself (see again Figure 2) shows the mechanical analog of this anisotropy, with P_{xx} greatly exceeding P_{yy} . Note that the lower pressure in Figure 2, the Hugoniot pressure, is a set of equilibrium values, $(P_{xx} + P_{yy})/2$. It is noteworthy that the height of the temperature maximum is sensitive to the definition of the local velocity. Evidently a temperature based on the local velocity, near the particle in question, and with a coarser averaging range $h = 3$, gives a smaller gradient and should accordingly provide a much simpler modeling challenge.

IV. SUMMARY

This work shows that planar shockwaves are stable for a smooth repulsive potential in a dense fluid. We also find that a mechanical instability makes the configurational temperature quite useless for such problems. Our investigation of temperature definitions

Figure 7

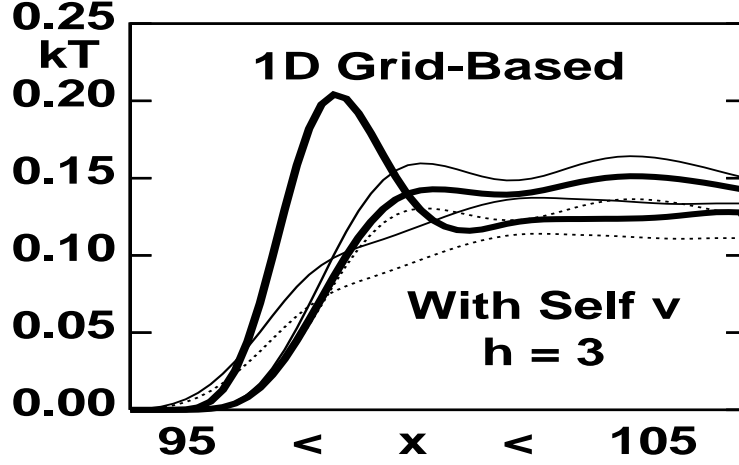


Figure 7: Typical instantaneous temperature profiles, at $t = 5Dt$ for the strong shockwave described in the text. Local particle-based definitions of stream velocity give the two somewhat lower temperature pairs, (T_{xx}^K, T_{yy}^K) . The grid-based definitions of T_{xx}^K and T_{yy}^K are indicated with the heaviest lines. They both use a one-dimensional weight function. This definition gives a strong temperature maximum for T_{xx}^K . In all three cases the longitudinal temperature T_{xx}^K exceeds the transverse temperature T_{yy}^K near the shock front. The temperatures obtained with two-dimensional weights and including the “self” terms in the average velocity are indicated by the dashed lines and are significantly lower than the rest throughout the hot fluid exiting the shockwave. The “correct” hot temperature, far from the shock, is $kT = 0.13$, based on separate equilibrium molecular dynamics simulations. The profiles shown here were all computed from the instantaneous state of the system after a simulation time of $5Dt = 200/u_s$.

shows that relatively smooth instantaneous temperature profiles can be based on the weight functions used in smooth particle applied mechanics. It is noteworthy that the constitutive relations describing inhomogeneous nonequilibrium systems must necessarily include an averaging recipe for the constitutive properties. The present work supports the idea¹¹ that the range of smooth averages should be at least a few particle diameters.

The better behavior of a particle-based temperature when the “self” terms are left out is not magic. Consider the equilibrium case of a motionless fluid at kinetic temperature T . The temperature of a particle in such a system should be measured in a motionless frame. If the “self” velocity is included in determining the frame velocity an unnecessary

Figure 8

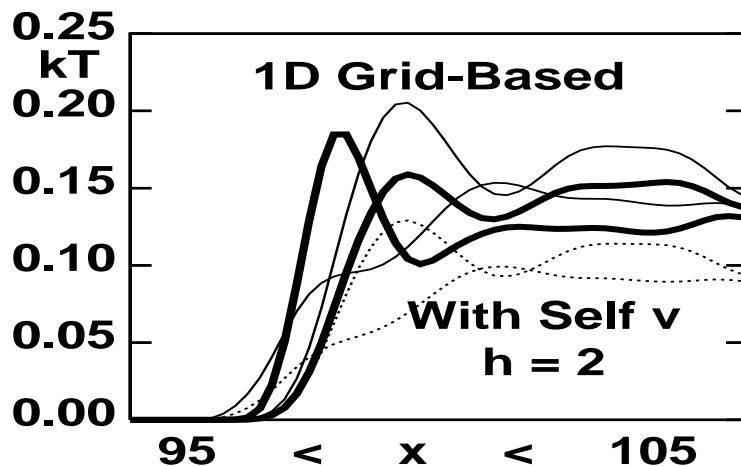


Figure 8: Temperature profiles with the same data as in Figure 7, but with a reduced averaging range, $h = 2$. Again, the temperatures including “self” contributions to the local velocity are shown as dashed lines. Notice the sensitivity of the maximum in T_{xx}^K to the range h . Far to the right, the “correct” hot temperature, at equilibrium, away from the shock, is $kT = 0.13$, based on separate equilibrium molecular dynamics simulations.

error will occur. Thus it is plausible that the “self” terms should be left out. The data shown in Figs. 7 and 8 support this view.

The instantaneous particle-based velocity average provides a smoother gentler profile which should be simpler to model. By using an elliptical weight function, much wider in the y direction than the x , one could consider the grid-based temperature as a limiting case. The somewhat smoother behavior of the particle-based temperature recommends against taking this limit. The elliptical weight function would leave the divergent configurational temperature unchanged.

V. ACKNOWLEDGMENT

We thank Brad Lee Holian for insightful comments on an early version of the manuscript. The comments made by the two referees were helpful in clarifying the temperature concept and its relation to earlier work. John Hardy was particularly forthcoming and generous in discussing the early history of his approach to making “continuum predictions from molecular dynamics simulations”. This work was partially supported by

the British Engineering and Physical Sciences Research Council and was presented at Warwick in the spring of 2009.

- ¹ G. E. Duvall and R. A. Graham, “Phase Transitions under Shockwave Loading”, *Reviews of Modern Physics* **49**, 523-577 (1971).
- ² L. D. Landau and E. M. Lifshitz, *Fluid Mechanics* (Reed, Oxford, 2000).
- ³ G. I. Kanel, W. F. Razorenov, and V. E. Fortov, *Shockwave Phenomena and the Properties of Condensed Matter* (Springer, Berlin, 2004).
- ⁴ W. J. Nellis, “P. W. Bridgman Contributions to the Foundations of Shock Compression of Condensed Matter” arXiv:0906.0106.
- ⁵ R. E. Duff, W. H. Gust, E. B. Royce, M. Ross, A. C. Mitchell, R. N. Keeler, and W. G. Hoover, in *Behavior of Dense Media under High Dynamics Pressures*, Proceedings of the 1967 Paris Conference (Gordon and Breach, New York, 1968).
- ⁶ V. Y. Klimenko and A. N. Dremin, in *Detonatsiya, Chernogolovka*, edited by G. N. Breusov *et alii* (Akademia Nauk, Moscow, 1978), page 79.
- ⁷ W. G. Hoover, “Structure of a Shockwave Front in a Liquid”, *Physical Review Letters* **42**, 1531-1534 (1979).
- ⁸ B. L. Holian, W. G. Hoover, B. Moran, and G. K. Straub, “Shockwave Structure *via* Nonequilibrium Molecular Dynamics and Navier-Stokes Continuum Mechanics”, *Physical Review A* **22**, 2798-2808 (1980).
- ⁹ J. Hardy, “Formulas for Determining Local Properties in Molecular-Dynamics Simulations: Shockwaves”, *Journal of Chemical Physics* **76**, 622-628 (1982), said by Hardy (private communication to WGH, June 2009) to be inspired by a 1963 conversation with Philippe Choquard (Lausanne) at the Lattice Dynamics Conference in Copenhagen.
- ¹⁰ O. Kum, Wm. G. Hoover, and C. G. Hoover, “Temperature Maxima in Stable Two-Dimensional Shock Waves”, *Physical Review E* **56**, 462-465 (1997).
- ¹¹ S. Root, R. J. Hardy, and D. R. Swanson, “Continuum Predictions from Molecular Dynamics Simulations: Shockwaves”, *Journal of Chemical Physics* **118**, 3161-3165 (2003).
- ¹² C. E. Ragan III, “Ultra-high-Pressure Shockwave Experiments”, *Physical Review A* **21**, 458-463 (1980).

- ¹³ H. M. Mott-Smith, “The Solution of the Boltzmann Equation for a Shockwave”, *Physical Review* **82**, 885-892 (1951)
- ¹⁴ O. G. Jepps, Ph. D. thesis, Australian National University (Canberra, 2001).
- ¹⁵ C. Braga and K. P. Travis, “A Configurational Temperature Nosé-Hoover Thermostat”, *Journal of Chemical Physics* **123** 134101 (2005).
- ¹⁶ Wm. G. Hoover and C. G. Hoover, “Nonequilibrium Temperature and Thermometry in Heat-Conducting Phi-4 Models”, *Physical Review E* **77**, 041104 (2008).
- ¹⁷ Wm. G. Hoover and C. G. Hoover, ”Nonlinear Stresses and Temperatures in Transient Adiabatic and Shear Flows *via* Nonequilibrium Molecular Dynamics”, *Physical Review E* **79**, 046705 (2009).
- ¹⁸ B. D. Butler, G. Ayton, O. G. Jepps and D. J. Evans, “Configurational Temperature: Verification of Monte Carlo Simulations”, *Journal of Chemical Physics* **109**, 6519-6522 (1998).
- ¹⁹ Wm. G. Hoover, C. G. Hoover, and J. F. Lutsko, “Microscopic and Macroscopic Stress with Gravitational and Rotational Forces, *Physical Review E* **79**, 0367098 (2009).
- ²⁰ L. B. Lucy, “A Numerical Approach to the Testing of the Fission Hypothesis”, *The Astrophysical Journal* **82**, 1013-1024 (1977).
- ²¹ Wm. G. Hoover, *Smooth Particle Applied Mechanics — The State of the Art* (World Scientific Publishers, Singapore, 2006, available from the publisher at the publisher’s site <http://www.worldscibooks.com/mathematics/6218.html>).
- ²² Wm. G. Hoover, *Computational Statistical Mechanics* (Elsevier, Amsterdam, 1991, available at the homepage <http://williamhoover.info/book.pdf>).
- ²³ W. G. Hoover, B. L. Holian, and H. A. Posch, “Comment I on ‘Possible Experiment to Check the Reality of a Nonequilibrium Temperature ’”, *Physical Review E* **48**, 3196-31998 (1993).
- ²⁴ Wm. G. Hoover and C. G. Hoover, “Single-Speed Molecular Dynamics of Hard Parallel Squares and Cubes”, arXiv:0905.0293. (submitted, *Journal of Statistical Physics*, 2009).
- ²⁵ L. D. Landau and E. M. Lifshitz, *Statistical Physics* (Muir, Moscow, 1951)(in Russian), Eq. 33.14.
- ²⁶ B. L. Holian, C. W. Patterson, M. Mareschal, and E. Salomons, “Modeling Shockwaves in an Ideal Gas: Going Beyond the Navier-Stokes Level”, *Physical Review E* **47**, R24-R27 (1993).
- ²⁷ B. L. Holian, “Modeling Shockwave Deformation *via* Molecular Dynamics”, *Physical Review A* **37**, 2562-2568 (1988).

